Study of charged particles emitted from ^{117}Te compound nuclei. II. Comparison between ^{40}Ar + ^{77}Se and ^{14}N + ^{103}Rh reactions and determination of critical angular momenta

J. Galin, B. Gatty, D. Guerreau, C. Rousset, U. C. Schlotthauer-Voos,* and X. Tarrago
Laboratoire de Chimie Nucléaire, Institut de Physique Nucléaire, 91406 Orsay, France

(Received 16 July 1973)

The compound nucleus ^{117}Te was formed with ^{14}N + ^{103}Rh at 71- and 107-MeV excitation energies. The deexcitation by protons, deuterons, tritons, and α particles was studied and compared to the deexcitation of the same compound nucleus ^{117}Te issued from ^{40}Ar + ^{77}Se at the same excitation energies. The influence of angular momentum on the evaporation mechanism (angular distributions and cross sections of charged particles) have allowed to determine different values of critical angular momenta limiting compound-nucleus formation. These values are discussed with respect to different models.

[NUCLEAR REACTIONS ^{103}Rh(^{14}N, ^{14}N); $E = 81$, 121 MeV; measured $\sigma(\theta)$; optical-model analysis ^{103}Rh(^{14}N,p), (^{14}N,d), (^{14}N,t), (^{14}N,α); $E = 81$, 121 MeV measured $\sigma(E, E_{\text{particle}})$, $\sigma(E_{\text{particle}}, \theta)$, σ_{particle}; discussion with regard to statistical model; comparison with Ar-induced reactions; deduced critical angular momenta.]

1. INTRODUCTION

The most characteristic feature of charged-particle evaporation in heavy-ion-induced compound-nuclear reactions, involving large angular momenta at medium excitation energies, is the very anisotropic emission of these particles.[1-5] The theoretical aspects of angular distributions have been previously discussed in detail in relation to experimental result for Ar-induced compound-nuclear reactions.[1] The main characteristics should, however, be recalled:

The angular distributions are symmetric with an anisotropy, which is determined by Jl/σ_v^2 and consequently depends on the population distributions of the compound nucleus (J and l being the spin of the compound-nucleus state and the angular momentum of the emitted particle, respectively, σ_v the classical spin cutoff parameter); the anisotropy increases with larger J and l but decreases slowly with higher excitation energy of the residual nucleus. Thus the anisotropies of the angular distributions allow one to determine the angular momentum distributions of the entrance channel leading to compound-nucleus formation.

Liquid-drop-model calculations[6-8] and various cross section measurements[9-14] have postulated the existence of a critical angular momentum J_{crit} for complete fusion; partial waves with $J < J_{\text{crit}}$ lead to compound-nucleus formation, while partial waves with $J > J_{\text{crit}}$ give rise only to direct interactions. The value of J_{crit} should be determined by a possible maximum deformation of the compound nucleus[6] or by a vanishing fission barrier.[7,8] Such a critical angular momentum is quantitatively related to the anisotropies of the angular distributions. As a consequence, angular distributions and cross section measurements of emitted particles allow one to study the evaporation mechanism as well as complete fusion cross sections.

In a recent experiment, the formation of the compound nucleus ^{117}Te by ^{40}Ar + ^{77}Se at excitation energies of 71 and 107 MeV with maximum relative angular momenta in the entrance channel of about $70\hbar$ and $110\hbar$ was investigated as well as its decay by protons, deuterons, tritons, α particles, and lithium.[1] It was found that the population distributions of the compound nucleus were different at the two excitation energies; at 71-MeV compound nucleus spins up to at least $50\hbar$ at 107 MeV up to at least $70\hbar$ had to be considered. It was concluded that if J_{crit} exists, J_{crit} (71 MeV) $\gtrsim 50\hbar$ and J_{crit} (107 MeV) $\gtrsim 70\hbar$.

Furthermore, these experiments showed that large angular momenta preferentially affect the evaporation of α particles, favoring in general the emission of high-energy α particles, as has already been indicated by compound-nuclear reactions induced by lighter projectiles.[5,15-19] However, this behavior was found to change for states near the yrast line, which have a decreasing emission probability for high-energy α particles.[1]

For further studies, it seems to be interesting to form the compound nucleus ^{117}Te at the same excitation energies as before but with different angular momentum distributions in the entrance

channels, in order to deduce more quantitatively the effects of angular momentum and to obtain more specific information especially on states near the yrast line and the critical angular momentum. Similar experiments were performed by Reedy *et al.*[19] with reactions induced by lighter projectiles, and it was found that a quantitative separation of different angular momentum regions is possible.

In the present study therefore, the reaction ^{14}N on ^{103}Rh with center-of-mass energies of about $E_{c.m.}=71$ and 107 MeV was used to give the compound nucleus ^{117}Te at the same excitation energies as before. Again cross sections, energy spectra, and angular distributions of the emitted charged particles have been measured. They will be discussed in comparison with the results of the ^{40}Ar-induced reactions in terms of the influence of angular momentum on evaporation mechanism and complete fusion cross sections.

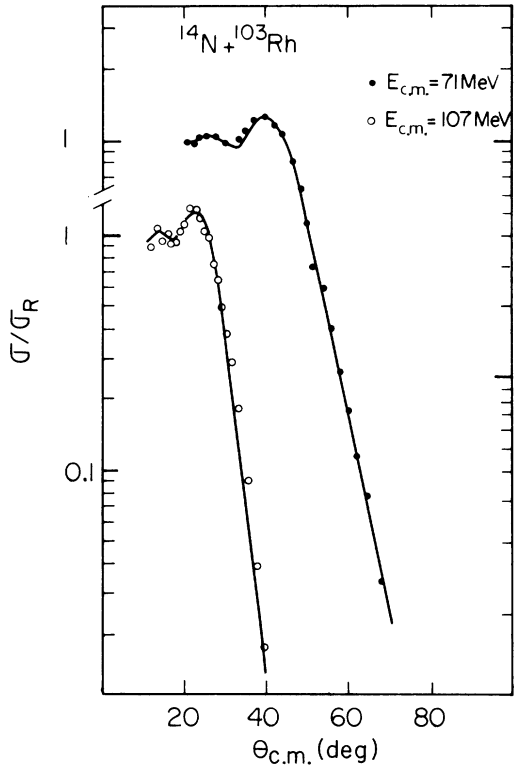

FIG. 1. Angular distributions of the elastic scattering of ^{14}N on ^{103}Rh; V_0 and W_0 are the depths of the real and imaginary potentials; r_{0R} and r_{0I}, the radius parameters, a_R and a_I, the corresponding diffuseness. The potential radii are given by $R_{R/I}=r_{0R/I}(A_T^{1/3}+A_p^{1/3})$, where A_T and A_p are the mass numbers of target and projectile; r_{0C} corresponds to the Coulomb potential: $V_0=41.8$ MeV, $r_{0R}=1.2$ fm, $a_R=0.49$ fm, $W_0=16.4$ MeV, $r_{0i}=1.22$ fm, $a_i=0.49$ fm, $r_{0c}=1.2$ fm.

2. ELASTIC SCATTERING

In order to obtain the angular momentum distributions in the entrance channels, the angular distributions of the elastic scattering were measured and described by a conventional optical model, using the optical-model code ABACUS II[+ 20] (Fig. 1). For both the real and imaginary potential a Woods-Saxon form factor was chosen. The optical potentials for the calculations in Fig. 1 are strongly absorbing and are the same for the two excitation energies. The parameters are only slightly different from those used by Auerbach and Porter for the description of the elastic scattering induced by ^{12}C, ^{14}N, and ^{16}O on various targets from Al to Au.[21]

The resulting transmission coefficients T_J are presented in Fig. 2, together with those obtained in the Ar case; furthermore the total reaction cross sections $\sigma_R=\pi\lambda\!\!\!^{-2}\sum_J(2J+1)\,T_J$ are given, where $\lambda\!\!\!^{-}$ is the reduced wave length of the incident channel. The angular momenta J_0, where $T_{J_0}=0.5$ are, at the lower excitation energy, $J_0(^{14}\text{N})=40\hbar$ and $J_0(^{40}\text{Ar})=56\hbar$, differing by $16\hbar$, and, at the higher excitation energy, $J_0(^{14}\text{N})=60\hbar$ and $J_0(^{40}\text{Ar})=93\hbar$ with the large difference of $33\hbar$. They are, however, about the same for the N-induced reaction at the higher excitation energy and the Ar-induced reaction at the lower one. Thus the comparison of the four reactions should give definite information on the influence of angular momentum, compound-nucleus spin, and excitation energy.

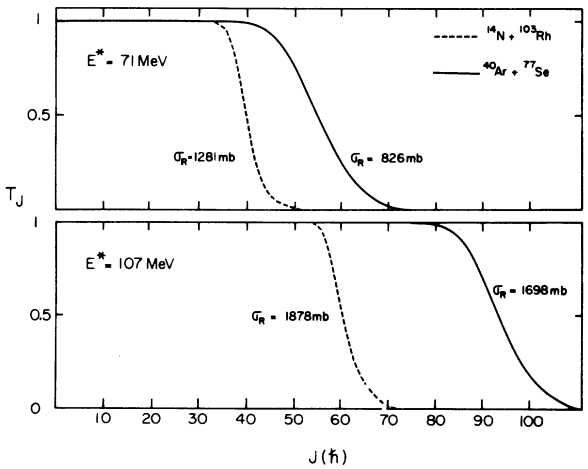

FIG. 2. Transmission coefficients for the investigated ^{14}N- and ^{40}Ar-induced reactions leading to the compound nucleus ^{117}Te at excitation energies of $E^*=71$ MeV and $E^*=107$ MeV. σ_R are the corresponding total reaction cross sections.

3. EXPERIMENTAL TECHNIQUE

The experiments were performed at the Orsay energy-variable cyclotron with a 82-MeV $^{14}N^{4+}$ beam of 200 nA and a 122.5-MeV $^{14}N^{5+}$ beam of 50 nA. The targets were self-supporting ^{103}Rh foils,[22] prepared by a cold rolling technique, with a thickness of 1.64 mg/cm^2. The laboratory energies in the middle of the target were about 81 and 121 MeV, which in this paper will be called the incident energies. They correspond to center-of-mass energies of 71 and 107 MeV, giving excitation energies in the ^{117}Te compound nucleus of 71 ± 1.5 and 107 ± 2.4 MeV, respectively. The experiments were performed in the same way as discussed earlier.[1]

4. COMPOUND-NUCLEUS RESULTS AND DISCUSSION

In order to obtain information about the influence of angular momentum and excitation energy on compound-nucleus formation and decay, the measured energy spectra, angular distributions, and cross sections of the ^{14}N-induced reactions will be presented and discussed in comparison with the results of the ^{40}Ar-induced reactions.[1]

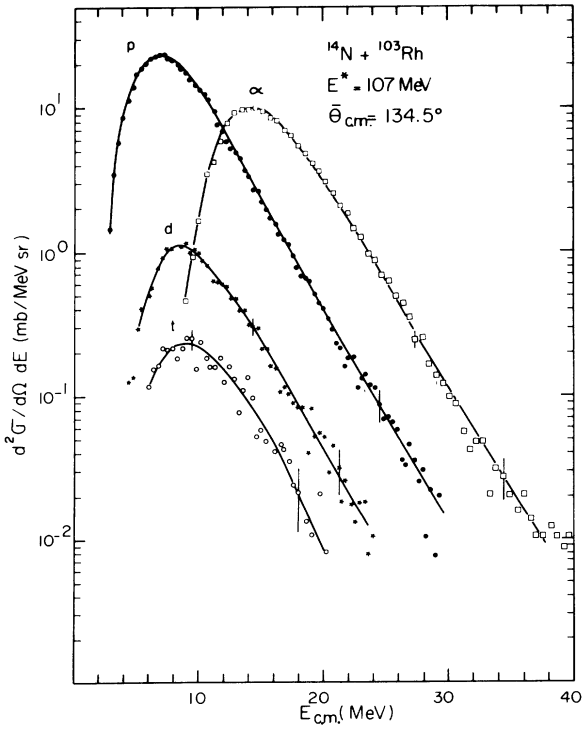

FIG. 3. ^{14}N-induced center-of-mass energy spectra of the charged particles emitted from the compound nucleus at the higher excitation energy, $E^* = 107$ MeV.

A. Charged-particle spectra

Center-of-mass energy spectra of the protons, deuterons, tritons, and α particles emitted from the ^{117}Te compound nucleus formed at the higher excitation energy by $^{14}N + ^{103}Rh$ are shown in Fig. 3. As in the ^{40}Ar-case they all exhibit the typical form of evaporation spectra.

In the ^{40}Ar-induced reaction at the higher excitation energy, a dependence of the average α-particle energy on the emission angle was observed. The distribution of the average energy versus the angles was found to be anisotropic and symmetric around $\theta_{c.m.} = 90°$, as predicted by the statistical theory of Ericson[2] for very high spin states in the compound nucleus. This effect is significantly less pronounced for α particles in the ^{14}N-induced reaction at the highest energy. It could not be observed within the experimental errors for α par-

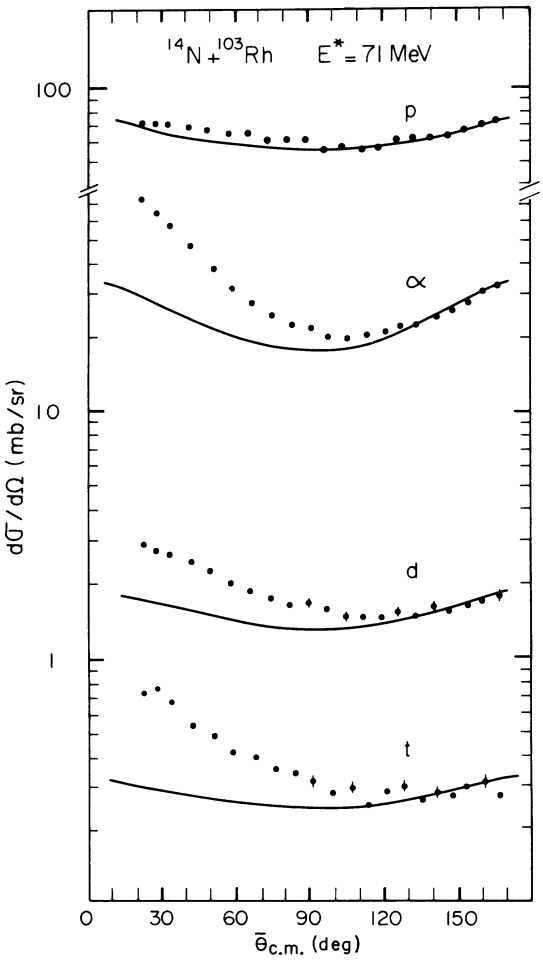

FIG. 4. ^{14}N-induced proton, deuteron, triton, and α-particle angular distributions integrated over all energies. The solid lines indicate the contribution of the compound-nuclear reaction; for details, see text.

ticles at the lower energy and protons at both excitation energies as in the ^{40}Ar case. In agreement with the interpretation given earlier, these results indicate that compound-nuclear states with larger spins are populated in the ^{40}Ar-induced reaction at the higher energy than in the other reactions. Furthermore it may be concluded that the influence of angular momentum on α-particle emission is more pronounced than on proton evaporation.

B. Angular distributions

1. *General aspects*

The angular distributions integrated over the total particle energies of the ^{14}N-induced reactions are presented in Figs. 4 and 5. In contrast to the ^{40}Ar-induced reactions where the angular distributions are symmetric around $\theta_{c.m.} = 90°$, in ^{14}N-induced reactions α-particle, triton, and deuteron angular distributions exhibit large forward-peaked contributions, which become more important and decrease rapidly at the higher incident energy. For protons, this effect is much smaller, but also exists. These components are normally attributed to direct interactions and should arise preferentially from the high-energy part of the particle spectra.

The energy dependence of proton and α-particle angular distributions integrated over small ranges of the particle kinetic energies are presented in Figs. 6 and 7 for the higher excitation energy. Indeed, it is found that the contributions of the direct component are less important at the lower particle energies but become significant for larger ones.

In order to separate the contributions of com-

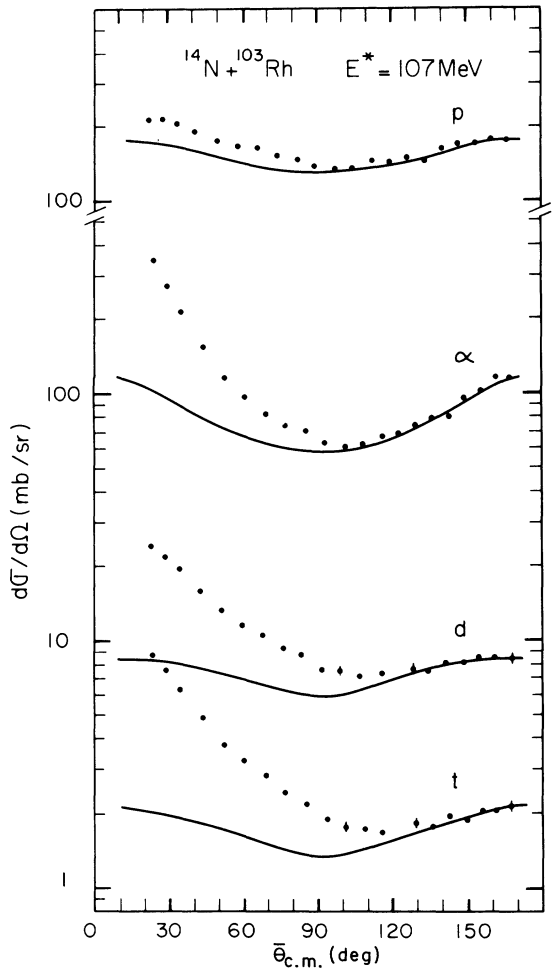

FIG. 5. ^{14}N-induced proton, deuteron, triton, and α-particle angular distributions integrated over all energies. The solid lines indicate the contribution of the compound-nuclear reaction; for details, see text.

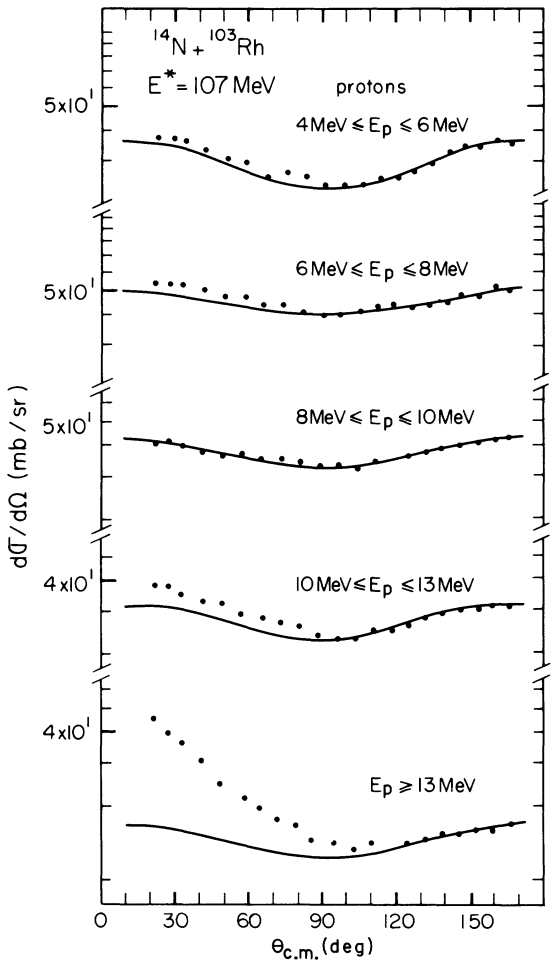

FIG. 6. ^{14}N-induced proton and α-particle angular distributions at the higher excitation energy integrated over small ranges of the particles' kinetic energy. The solid lines indicate the contribution of the compound-nuclear reaction; for details, see text.

pound nucleus and direct interactions, the following procedure was applied: The experimental angular distributions at very backward angles could be attributed to the compound nucleus alone. The direct contributions at the very forward angles were obtained as the difference between the experimental cross sections at these angles and the compound-nucleus cross section at the corresponding backward angles. These direct-reaction cross sections versus the emission angle are found to follow a straight line on a semilogarithmic scale and as a consequence the direct contributions at larger angles are assumed to continue this behavior. Thus, the probable compound-nuclear cross sections around $\theta_{c.m.} = 90°$ may be deduced. Least-square fits, using a sum over even Legendre polynomials, were performed for the compound-nuclear cross sections deduced for angles $\theta_{c.m.} > 90°$, in order to obtain the probable compound-nuclear angular distributions. The solid lines in Figs. 4–7 are drawn to indicate this part of the reaction. From these fits the anisotropies $\sigma_{0°}/\sigma_{90°}$ were deduced. The values for the angular distributions integrated over the total particle energies are given in Table I and compared to those of the Ar-induced reactions.

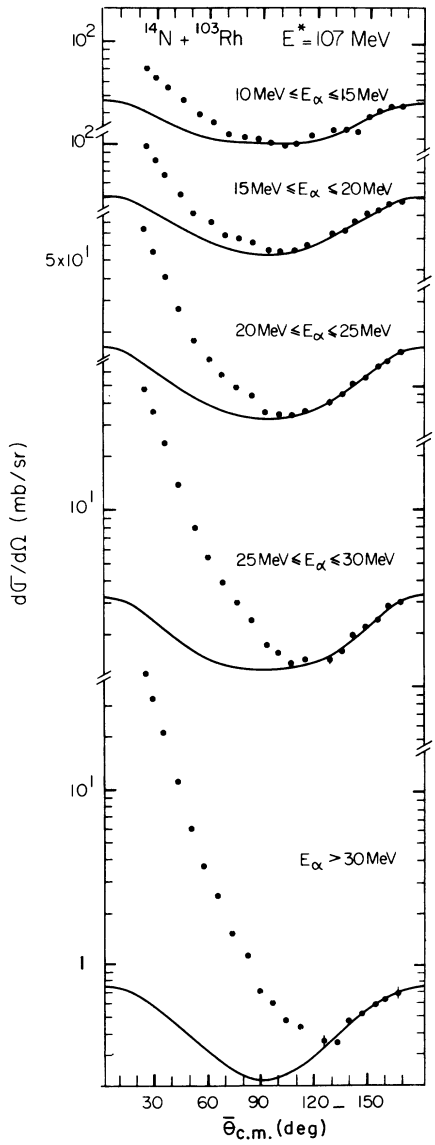

FIG. 7. ^{14}N-induced proton and α-particle angular distributions at the higher excitation energy integrated over small ranges of the particles' kinetic energy. The solid lines indicate the contribution of the compound-nuclear reaction; for details, see text.

At each excitation energy it is found that the absolute anisotropies are larger in the ^{40}Ar case, indicating that the colliding nuclei $^{40}Ar + ^{77}Se$ populate compound-nuclear states with larger spins than do the incident particles $^{14}N + ^{103}Rh$. On the other hand, the anisotropies of proton and α-particle angular distributions are constant or even increase with the excitation energy of the compound nucleus in the ^{40}Ar-induced reactions as well as in the ^{14}N cases, indicating that larger angular momenta are reached at the higher excitation energy. This variation is more significant for α particles than for protons, showing that angular momentum affects mainly the evaporation of α particles. These results had already been reflected in the angular dependence of the average kinetic particle energies. As a consequence, it may be concluded that the spin distributions populated in the compound nucleus depend significantly on the incident channel and the excitation energy.

2. *Theoretical description*

Liquid-drop-model predictions,[6-8] based on calculations of either the maximum possible deformation of the compound nucleus[6] or the angular momentum, where the fission barrier vanishes,[7,8] have indicated the existence of a critical angular momentum J_{crit}, above which the partial waves of the entrance channel do not contribute to compound-nucleus formation. Moreover the existence of a critical angular momentum for compound-nucleus formation was qualitatively verified by several cross-section measurements.[9-14]

However, this effect should also be reflected in the angular distributions, as they depend on the angular momentum distributions of the incident channels. As shown by the discussion of the anisotropies, the population distributions of the compound nuclei in the reactions under study are certainly different for the ^{14}N- and ^{40}Ar-induced reactions and depend also on the excitation energy.

TABLE I. Anisotropies $\sigma_{0°}/\sigma_{90°}$ of the angular distributions, integrated over the total energy spectra.

		$E^*=71$ MeV	$E^*=107$ MeV
P	$^{14}N+^{103}Rh$	1.32 ± 0.13	1.34 ± 0.13
	$^{40}Ar+^{77}Se$	1.43 ± 0.10	1.53 ± 0.11
α	$^{14}N+^{103}Rh$	1.87 ± 0.19	1.94 ± 0.19
	$^{40}Ar+^{77}Se$	2.53 ± 0.20	3.16 ± 0.15

In order to investigate this problem quantitatively the angular distributions of the high-energy particles which should arise preferentially from the first evaporation step were described with the statistical theory of Ericson.[2] It was found by a complete calculation for the whole evaporation cascade, which will be discussed in a further publication, that protons with $E_p \geq 13$ MeV and α particles with $E_\alpha \geq 25$ MeV may be considered to a good approximation as being due to the first evaporation step (Fig. 8). Thus the angular-distribution calculations were performed for these particles, taking different angular momentum cutoffs

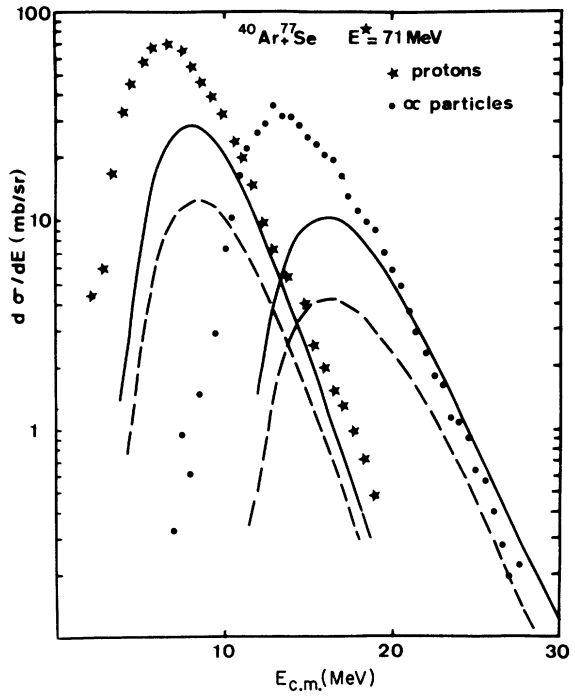

FIG. 8. Comparison between the measured p and α-particle spectra integrated over θ and the results of a statistical calculation using GROGI2 computer code. The dashed lines exhibit the part of the spectra issued from a first step and the solid line, the part of the spectra issued from either a first step or just after one-neutron evaporation. The following parameters have been used in the calculation and will be discussed in a future publication: $a=A/6$, $\Gamma_\gamma=0.1$ eV, $J_{crit}=52\hbar$, $\mathcal{I}=\mathcal{I}_{rig}$. Shell effects have been introduced.

J_{co} in the incident channels into account. The free parameters of the theory were chosen as previously discussed,[1] with the moment of inertia being equal to the moment of inertia of a rigid body $\mathcal{I}=\mathcal{I}_{rig}$; density parameters of $a=A/6$ and $a=A/8$, where A is the mass number of the nucleus under consideration, were found to give the same results within the experimental errors. The transmission coefficients in the exit channels were calculated by the optical-model code ABACUS 2,[20] taking for protons the potentials given by Mani, Melkanoff, and Iori[23] and for alpha particles those given by Huizenga and Igo.[24]

a. ^{14}N on ^{103}Rh. Results for the α particles evaporated in the ^{14}N-induced reaction at 107-MeV excitation energies are shown in Fig. 9. A value of $J_{co}=62\hbar$, which is about the same as the value J_0 defined earlier gives too large anisotropies. In order to test the influence of the critical angular momentum, calculations in steps of $10\hbar$ were performed. A value of $J_{co}=42\hbar$ results in too weak anisotropies as compared to the experimental data, whereas a good description of the angular distributions is found with $J_{co}=52\hbar$. With this value also the proton angular distribution from the same excitation energy is well described (Fig. 9). Thus in the present case the compound nu-

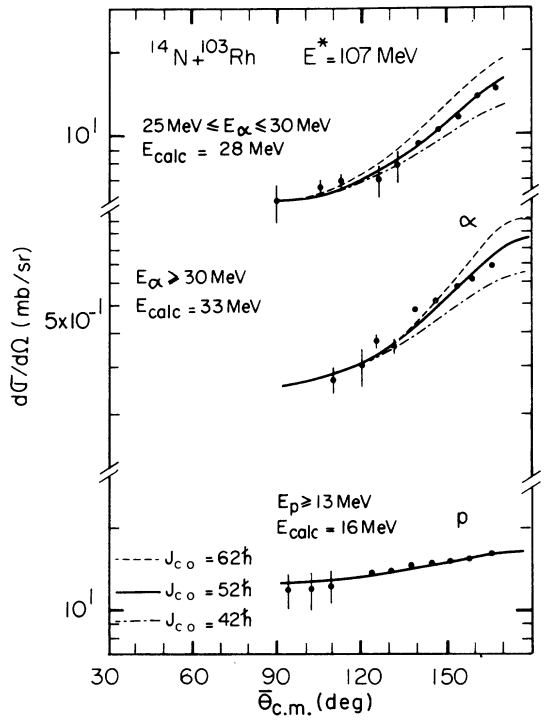

FIG. 9. Predictions of angular distributions with the statistical theory for the first-step emission of protons and α particles with different "angular momentum cutoff" in the entrance channel, J_{co}.

cleus was formed with a maximum spin of about $52\hbar$, which is much smaller than the angular momentum brought in by the entrance channel. Consequently the existence of J_{crit} for compound-nucleus formation in the reaction ^{14}N on ^{103}Rh at the higher energy is verified and its value is found to be $52\hbar \pm 5\hbar$.

It was shown in the discussion of the anisotropies that the maximum angular momentum leading to compound-nucleus formation is smaller at the lower excitation energy than at the higher one. Consequently the critical angular momentum for the ^{14}N-induced compound-nucleus formation at $E_{c.m.} = 71$ MeV is $J_{crit} < 50\hbar$. Calculations with different cutoff values in the angular momentum distribution of the incident channel J_{co} were performed for the high-energy α-particle angular distributions (Fig. 10). A value of $J_{co} = 32\hbar$ gives a too weak anisotropy, while a good description of α-particle and proton angular distributions is obtained with $J_{co} = 40\hbar$ (Fig. 10). Unfortunately, even larger values of J_{co} do not increase the calculated anisotropies significantly, as the transmission coefficients are already very small in this angular momentum region (see Fig. 2). However, direct-reaction cross-section measurements in the reaction ^{14}N on Ag at a slightly smaller excitation energy have shown that $J_{crit} < 36\hbar$.[12] Thus, a value of $J_{crit} \sim 40\hbar \pm 5\hbar$ seems physically reasonable in the $^{14}N + ^{103}Rh$ reaction at the lower excitation energy.

b. ^{40}Ar on ^{77}Se. In the ^{40}Ar-induced reactions, however, only lower limits for the values of J_{crit} could be deduced. They were found to be $J_{crit} \gtrsim 50\hbar$ at 71-MeV and $J_{crit} \gtrsim 70\hbar$ at 107-MeV excitation energies. Calculations with higher compound-nucleus spins showed that the anisotropies remained considerably constant. This effect was explained by the influence of the yrast line, the transmission coefficients being still sufficiently large in the angular momentum region under consideration.

In order to illuminate this point, the emission of 30-MeV α particles from the compound nucleus at both excitation energies is considered, leading to states of about 40- and 75-MeV excitation energies in the residual nuclei. The corresponding yrast levels have angular momenta of about $55\hbar$ and $75\hbar$, respectively. Thus, the evaporation of high-energy α particles from compound-nuclear states with very large spin is expected to be hindered by the yrast levels in the residual nucleus.

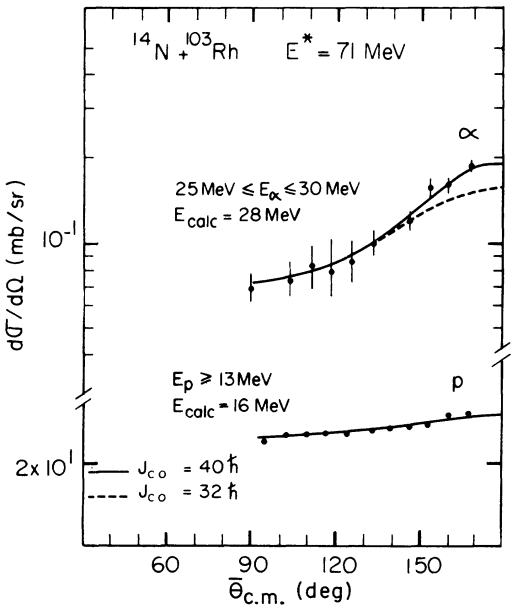

FIG. 10. Predictions of angular distributions with the statistical theory for the first-step emission of protons and α particles with different "angular momentum cutoff" in the entrance channel, J_{co}.

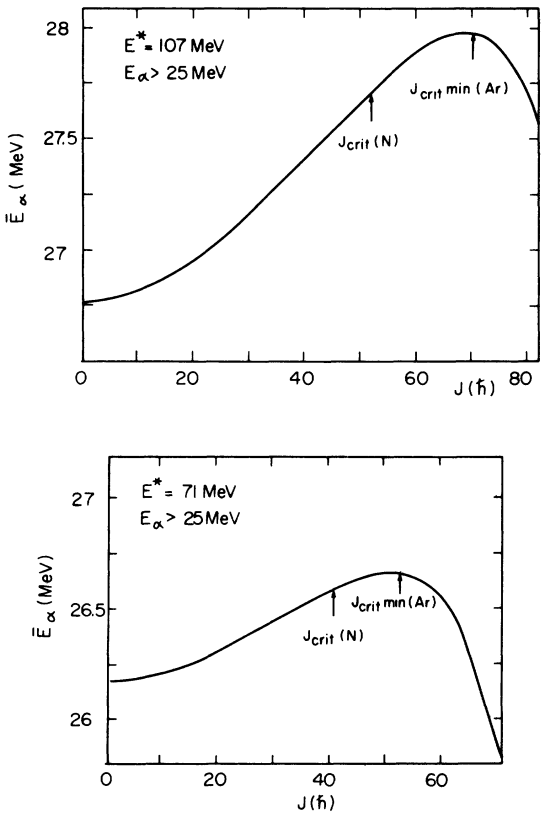

FIG. 11. Dependence on the compound-nucleus spin of the average kinetic energy $\bar{E}_\alpha$ of high-energy α particles ($E_\alpha > 25$ MeV) at both excitation energies.

Figure 11 shows the calculated average kinetic energy of the particles with an energy of $E_\alpha > 25$ MeV emitted during the first evaporation step from the compound nucleus at both excitation energies versus the compound-nucleus spin. The average energy increases significantly with angular momentum, but indeed passes a maximum at about $50\hbar$ and $70\hbar$ for the 71- and 107-MeV excitation energies, respectively, and decreases afterwards. Thus in general an enhancement of high-energy α-particle evaporation with the compound-nucleus spin can be observed, in agreement with earlier results[19,25]; for states near the yrast line, however, their emission probability drops significantly.

It is evident that, in the presented study, the influence of the yrast line is only observed in the ^{40}Ar cases and not in the ^{14}N ones. At the same excitation energies, the ^{14}N-induced reactions lead to compound-nuclear states with considerably smaller spins than do the ^{40}Ar-induced reactions, as indicated in Fig. 11, where the arrows correspond to the critical angular momenta in the ^{14}N cases and to the minimum critical angular momenta in the ^{40}Ar reactions, as deduced earlier.

3. *Anisotropies*

The variation of the anisotropies $\sigma_{0^\circ}/\sigma_{90^\circ}$ of proton and α-particle angular distributions with particle kinetic energy are presented for both the ^{14}N- and ^{40}Ar-induced reactions in Fig. 12. They were deduced from the solid lines describing the angular distributions integrated over small ranges of particle energy, examples of which were shown in Figs. 6 and 7.

The α-particle anisotropies increase with the particle energy for ^{40}Ar- and ^{14}N-induced reactions; however, in the ^{40}Ar case, they approach some constant values for energies $E_\alpha \gtrsim 30$ MeV, whereas they still increase in the ^{14}N case. This different behavior may be explained by the variation of the average α-particle energy with compound-nucleus spin as discussed in the previous chapter. It was shown that in general the emission of high-energy α particles is favored by a high compound-nucleus spin, but decreases for states near the yrast line. The observed effect in the anisotropies may be qualitatively reproduced by statistical model calculations of the first evaporation step for different particle energies (Fig. 12).

For protons, the anisotropies versus the proton kinetic energy are constant within the experimental errors, in accordance with the result that the proton average kinetic energy is only slightly affected by the compound-nucleus spin.

C. Cross sections

1. *General features*

The cross sections for proton, deuteron, triton, and α-particle emission in the ^{14}N-induced reactions are given in Table II. The values are integrated over all particle energies and emission

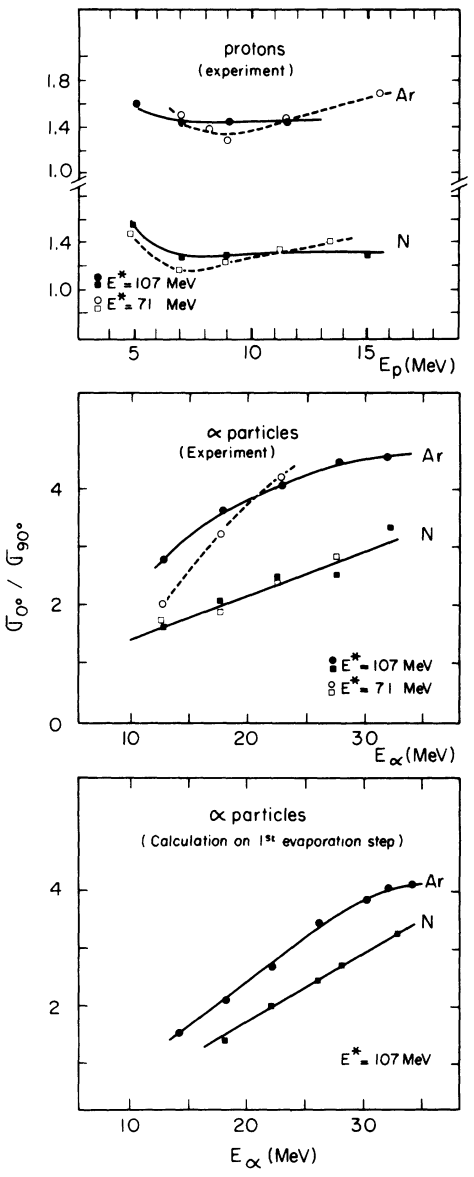

FIG. 12. Anisotropies $\sigma_{0^\circ}/\sigma_{90^\circ}$ of proton and α particle angular distributions. The upper part represents the experimental values of the ^{40}Ar- and ^{14}N-induced reactions at both excitation energies, obtained from the angular distributions integrated over small ranges of the particles' energy. The lower part shows calculations of the first evaporation step for α particles emitted in the ^{40}Ar- and ^{14}N-induced reactions at the high excitation energy.

TABLE II. Cross sections (mb), integrated over particle energies and emission angles, of the evaporated charged particles. σ_R is the total reaction cross section as calculated by the optical model.

	$^{40}Ar + ^{77}Se$			$^{14}N + ^{103}Rh$		
	$E^* = 71$ MeV	$E^* = 107$ MeV	σ_{107}/σ_{71}	$E^* = 71$ MeV	$E^* = 107$ MeV	σ_{107}/σ_{71}
p	410 ± 60	1090 ± 110	2.7	794 ± 80	1894 ± 190	2.3
d	8.5 ± 1.5	47 ± 10	5.5	18.4 ± 3.0	90 ± 14	4.9
t	1.5 ± 0.7	15 ± 5	10	3.5 ± 0.7	21 ± 3	6
α	207 ± 30	840 ± 90	4.1	266 ± 30	930 ± 90	3.5
σ_α/σ_p	0.51	0.77	1.51	0.34	0.49	1.49
σ_R	826	1698		1281	1878	

angles, taking only the evaporation part into account as indicated in the discussion of the angular distributions.

A significant increase of deuteron, triton, and α-particle cross section with the excitation energy is observed as in the ^{40}Ar case.[1] This behavior might be attributed to the strong influence of angular momentum, although, unfortunately, the effects of Coulomb barrier and binding energies should also favor the emission of tritons and α particles with increasing excitation energy. On the other hand, at each excitation energy, the values of σ_α/σ_p are larger for the ^{40}Ar case. They are, however, about the same for the ^{14}N-induced reactions at the higher energy and the ^{40}Ar-induced réaction at the lower excitation energy. For these two reactions, the angular momentum population distributions of the compound nucleus had been found to be very similar. These effects indicate that the emission probability of α-particles relative to that one of protons depends essentially on the compound-nucleus spin and increases with larger angular momentum.

2. Cross sections of compound-nucleus formation

According to the statistical theory, the cross section for the evaporation of a particle ν from a compound nucleus formed by entrance channel x is given by

$$\sigma(x, \nu) = \pi \lambda\!\!\!^{-}_x{}^2 \sum_J (2J+1)\, T_J(x)\, P_J^{(\nu)}, \qquad (1)$$

where $\pi \lambda\!\!\!^{-}_x{}^2 (2J+1)\, T_J(x)$ is the cross section for the formation of the compound nucleus with spin J; $\lambda\!\!\!^{-}_x$ is the reduced wave length and the $T_J(x)$ are the transmission coefficients in the entrance channel; $P_J^{(\nu)}$ is the probability for the emission of particle ν from this state.

With the comparison of the ^{14}N- and ^{40}Ar-induced reactions, a qualitative study of the cross sections in different angular momentum regions is possible, by applying a method first used by Reedy *et al.*[19] This method is based on the independence hypothesis of compound nucleus formation and decay, which was verified among others by Fluss *et al.*[26] and shown to be valid also for heavy-ion-induced reactions.[27]

Thus the emission probabilities $P_J^{(\nu)}$ of Eq. (1) are the same, when the same compound nucleus at the same excitation energy is formed by different entrance channels. Denoting the cross sections divided by $\lambda\!\!\!^{-}_x{}^2$ for the evaporation of particle ν from the compound nucleus ^{117}Te formed with $^{14}N + ^{103}Rh$ and $^{40}Ar + ^{77}Se$ by $\sigma_\nu(^{14}N)$ and $\sigma_\nu(^{40}Ar)$, respectively, it follows from Eq. (1) that

$$\sigma_\nu(^{40}Ar) - \sigma_\nu(^{14}N) = \sum_J (2J+1) P_J^{(\nu)} \times [T_J(^{40}Ar) - T_J(^{14}N)]. \qquad (2)$$

The left-hand side of Eq. (2) consists only of values which can be determined experimentally, while the right-hand side depends on the differences in the transmission coefficients leading to compound-nucleus formation in both reactions.

It turns out to be useful to distinguish three regions: (1) $\Delta T_J \equiv T_J(^{14}N) \neq 0$: In this region the evaporation cross sections are given by $\sigma_\nu(^{14}N)$; (2) $\Delta T_J \equiv T_J(^{40}Ar) \neq 0$: In this region they are given by $\sigma_\nu(^{40}Ar)$; (3) $\Delta T_J \equiv T_J(^{40}Ar) - T_J(^{14}N) \neq 0$: In this region they are determined by $\sigma_\nu(^{40}Ar) - \sigma_\nu(^{14}N)$. The quantities $(2J+1)\, T_J$ of each region, taking the whole angular momentum distributions of the incident channels into account, are given in Fig. 13, indicating that the average angular momentum increases from region (1) to (3), thus allowing the study of the dependence of cross sections on the compound-nucleus spin.

In the following all cross sections will be considered in units of $\lambda\!\!\!^{-}_x{}^2$. Table III shows for both excitation energies the average spins of each region, the cross sections σ_p and σ_α, and the total reaction cross sections σ_R. Furthermore the values σ_ν/σ_R and the quantities σ_{th}/σ_R are

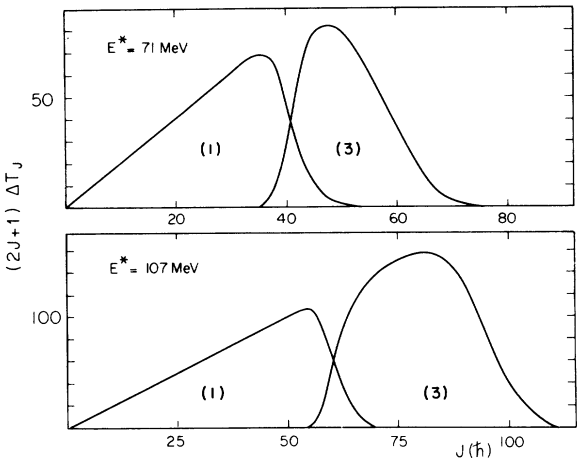

FIG. 13. The quantities $(2J+1)\Delta T_J$ taking the whole angular momentum distributions of the incident channel into account; the corresponding values in region 2 are the sum of those in regions 1 and 3; region 1 is defined by $\Delta T_J \equiv T_J(^{14}\mathrm{N}) \neq 0$, region 2 by $\Delta T_J \equiv T_J(^{40}\mathrm{Ar}) \neq 0$, and region 3 by $\Delta T_J \equiv T_J(^{40}\mathrm{Ar}) - T_J(^{14}\mathrm{N}) \neq 0$; for further details, see text.

given where $\sigma_{ch} = \sum \sigma_\nu$, $\nu = p, d, t, \alpha$ is the charged-particle cross section. At both excitation energies σ_{ch}/σ_R is found to become smaller with increasing average angular momentum. On the other hand, the total evaporation cross section σ_{ev} divided by the cross section for the compound-nucleus formation σ_{CN} should be a constant in the three regions. σ_{ev} is given by the cross section of charged-particle emission plus the evaporation cross section of neutrons, σ_n, plus the emission cross section for γ, σ_γ, and the fission cross section, σ_f:

$$\sigma_{ev} = \sigma_{ch} + \sigma_n + \sigma_\gamma + \sigma_f \ .$$

Fission studies with a ^{14}N beam of 126 MeV have shown that $\sigma_f = 0.4$ mb in the mass region under consideration [28]; similarly the cross section was found to be small in the fission induced by ^{40}Ar on Mo.[29] Thus in the present discussion σ_f may be neglected as compared to σ_{ch}.

The quantity $\sigma_\gamma/\sigma_{CN}$ may be assumed in a first approximation to be independent on the compound-nucleus spin. Calculations of Grover and Gilat[30] show that the γ-ray emission probability depends essentially on the neighborhood to the yrast line.

Furthermore theoretical calculations predict that the neutron-emission probability decreases slightly with the compound-nucleus spin.[25] Consequently, σ_{ch}/σ_{CN} is expected to be constant or to increase slightly with angular momentum. Thus the presented results imply, independently from the earlier discussion of the angular distributions,

TABLE III. Average compound-nucleus spin $\langle J \rangle$, calculated reaction cross sections σ_R, and various experimental cross sections in units of the square reduced wave lengths for regions 1, 2, and 3, taking the whole angular momentum distributions in the entrance channels with maximum value J_{max} into account; for further details, see text.

	$E^*=71$ MeV $J_{max}(^{14}\mathrm{N})=52\hbar$ $J_{max}(^{40}\mathrm{Ar})=72\hbar$			$E^*=107$ MeV $J_{max}(^{14}\mathrm{N})=72\hbar$ $J_{max}(^{40}\mathrm{Ar})=110\hbar$		
Region	1	2	3	1	2	3
$\langle J \rangle$	27.2	38.6	50	41.1	66.5	79
σ_R	540	995	455	1180	2820	1640
σ_α	112	250	138	585	1400	815
σ_p	335	494	159	1190	1820	630
σ_α/σ_R	0.208	0.251	0.304	0.50	0.50	0.50
σ_p/σ_R	0.62	0.498	0.350	1.01	0.64	0.38
σ_{ch}/σ_R	0.84	0.76	0.65	1.56	1.18	0.91

that the cross sections for the compound-nucleus formation σ_{CN} are smaller than the total reaction cross sections σ_R.

For the ^{14}N-induced reactions σ_{CN} is known from the analysis of the angular distributions. With the condition that σ_{ch}/σ_{CN} is independent of the compound-nucleus spin, an upper limit of the cross sections for the compound-nucleus formation by $^{40}\mathrm{Ar} + ^{77}\mathrm{Se}$ may be deduced and consequently an upper limit for the critical angular momenta.

With a $J_{crit}(^{14}\mathrm{N}) = 40\hbar$ at 71-MeV excitation energy there follows $J_{crit}(^{40}\mathrm{Ar}) < 52\hbar$; at 107-MeV excitation energy the value $J_{crit}(^{14}\mathrm{N}) = 52\hbar$ implies $J_{crit}(^{40}\mathrm{Ar}) < 70\hbar$. Combining these results with the study of the angular distributions it is found that $J_{crit}(^{40}\mathrm{Ar}, 71\ \mathrm{MeV}) \sim 50\hbar$ and $J_{crit}(^{40}\mathrm{Ar}, 107\ \mathrm{MeV}) \sim 70\hbar$.

TABLE IV. Average compound-nucleus spin $\langle J \rangle$, calculated cross sections for the compound-nucleus formation σ_{CN}, and various experimental cross sections in units of the square reduced wave lengths for regions 1, 2, and 3—as defined in the text—considering those angular momentum distributions in the entrance channels leading to compound nucleus formations and being determined by J_{crit}.

	$E^*=71$ MeV $J_{crit}(^{14}\mathrm{N})=40\hbar$ $J_{crit}(^{40}\mathrm{Ar})=52\hbar$			$E^*=107$ MeV $J_{crit}(^{14}\mathrm{N})=52\hbar$ $J_{crit}(^{40}\mathrm{Ar})=70\hbar$		
Region	1	2	3	1	2	3
$\langle J \rangle$	24.6	34.6	46	35.3	49.5	62.5
σ_{CN}	507	837	330	880	1585	705
$\sigma_\alpha/\sigma_{CN}$	0.21	0.30	0.42	0.67	0.88	1.15
σ_p/σ_{CN}	0.66	0.59	0.48	1.35	1.15	0.89
σ_d/σ_{CN}	0.014	0.010	0.005	0.06	0.05	0.03
σ_t/σ_{CN}				0.015	0.016	0.017
σ_{CN}/σ_R	0.94	0.84		0.75	0.56	

3. *Influence of the compound-nucleus spin on the evaporation cross section*

Some further conclusions concerning the evaporation mechanism may be drawn from this procedure. Table IV presents the cross sections for compound-nucleus formation in the three regions, obtained with the above given critical angular momenta, as function of the average compound-nucleus spin. Furthermore the values of σ_ν/σ_{CN} are given for protons, deuterons, tritons, and α particles.

At both excitation energies the relative emission probability of α particles increases significantly with the compound-nucleus spin, whereas the relative proton cross sections decrease slowly, in agreement with theoretical predictions of Williams and Thomas.[25] The same behavior for α particles was found at smaller angular momentum by Reedy *et al.*,[19] whereas in their experiment the proton cross sections remained constant within the experimental uncertainties.

With slightly increasing relative cross sections, the tritons exhibit an intermediate behavior. A physical explanation may be found in the fact that tritons and especially α particles can carry away larger angular momenta than do protons. Thus a compound nucleus excited at high spin states favors the emission of those particles which can diminish considerably the compound-nucleus spin. The relative deuteron emission probabilities, however, decrease even more strongly with angular momentum than do the relative proton cross sections. This effect cannot be explained in a coherent way with the other results.

5. COMPLETE FUSION CROSS SECTIONS AND CRITICAL ANGULAR MOMENTA

In heavy-ion-induced reactions the determination of complete fusion cross sections remains a crucial problem. The most important questions concern the existence of a critical angular momentum and its dependence on the masses of the colliding nuclei and on their relative energy or some other related parameter, i.e., the energy above the Coulomb barrier or the excitation energy of the compound system. Recently, Zebelman and Miller[14] have measured fusion cross sections for the same compound nucleus with three entrance channels; Natowitz *et al.*[11] have studied the influence of the incident energy on fusion cross sections.

In the presented studies the same compound nucleus was formed by two different reactions at two excitation energies and four values for J_{crit} could be determined (Table IV). It seems interesting to compare, at least qualitatively, these results to those of Zebelman and Miller and of Natowitz. The comparison might be all the more useful as the determination of the critical angular momenta are quite different. In the earlier experiments[11,14] complete fusion cross sections have been measured by solid track detectors and the corresponding J_{crit} have been deduced; in the present experiments, values of J_{crit} have been directly determined by an analysis of α-particle angular distributions.

Table IV reflects two tendencies. Considering the same projectile and target system, J_{crit} is found to increase with increasing energy (from $40\hbar$ to $52\hbar$ in ^{14}N induced reactions, from $50\hbar$ to $70\hbar$ in ^{40}Ar reactions). A similar variation was observed by Natowitz *et al.*[11] in bombarding Al, Ti, Ni, and Cu targets by ^{12}C ions at different energies. This behavior does not agree with the results of liquid-drop-model predictions; Kalinkin and Petkov,[6] calculating the maximum possible deformation of the compound nucleus, have postulated a decrease of the critical angular momentum with increasing energy; Cohen, Plasil, and Swiatecki[7] found, by the determination of the angular momentum where the fission barrier vanishes that J_{crit} should be independent of the excitation energy. Furthermore, the presented experimental results show that at a given excitation energy J_{crit} is larger with the heavier projectile, i.e., ^{40}Ar. A similar result has been reported by Zebelman and Miller.[14] Thus, the processes which compete with fusion are certainly not completely determined by the equilibrium properties of compound nucleus. Consequently Blann and Plasil's[8] formalism which is based on an equilibrium model taking into account fission competition during deexcitation of the compound nucleus is expected to give the energy dependence of J_{crit} but cannot reproduce completely the experimental results. On the other hand, a dynamic model based on the force equilibrium concept proposed by Wilczynski[31] shows a dependence of J_{crit} on the combination of target and projectile used for the production of the compound system. However, no energy dependence is given by this model. Another interpretation for the limitation of complete fusion processes could be connected to the existence of the yrast line. However, in the presented experiments a rough calculation of this line, taking into account the moment of inertia of a rigid body, leads to values of $75\hbar$ and $95\hbar$, respectively, for the lower and higher excitation energies, independently from the incident channel. Thus, no existing theory can completely explain the values of critical angular momenta measured in these experiments.

6. CONCLUSIONS

This study of charged particles emitted from ^{117}Te compound nuclei obtained by two different ways gives some answers on the role played by the angular momentum of the compound system in its deexcitation. It could be shown that α-particle emission depends strongly on the spin states of the compound nucleus. A significant increase of α-particle anisotropies with increasing particle kinetic energy was found. This effect indicates that high spin states favor the emission of high-energy α particles. However, as a new result, in Ar-induced reactions the anisotropies approach some constant values for the high-energy α particles. This effect reproduced by statistical model calculations of the first evaporation step indicates a strong influence of the yrast levels on the deexcitation of high-spin states. For these states the probability of evaporating high-energy α particles is very small. At the same excitation energies this effect was not observed in ^{14}N-induced reactions as the maximum spin of the compound nucleus was considerably smaller.

The other point which should be emphasized is the possibility of determining values of the critical angular momenta J_{crit} leading to compound-nucleus formation by an analysis of α-particle angular distributions. This is a new and sensitive method so long as the transmission coefficient corresponding to this J_{crit} is not too small and so long as the J_{crit} value for a given excitation energy is not too close to the corresponding yrast level. By this procedure and a study of charged-particle cross sections four values of J_{crit} have been obtained for the presented reactions. Introducing them into a complete statistical deexcitation calculation for the whole evaporation chain, a good description of the experimental energy spectra was obtained.[32]

The authors want to thank Professor M. Lefort for his continuous interest in this work, his support, and many helpful discussions. A critical reading of the manuscript by Dr. R. L. Hahn is gratefully acknowledged.

---

*On leave of absence from Physikalisches Institut der Universität, Marburg, Germany, supported by G. S. I., Darmstadt, Germany.

[1]J. Galin, B. Gatty, D. Guerreau, C. Rousset, U. Schlotthauer-Voos, and X. Tarrago, preceding paper, Phys. Rev. C 9, 1113 (1974).

[2]T. Ericson and V. Strutinsky, Nucl. Phys. 8, 284 (1958); 9, 689 (1959); T. Ericson, Adv. Phys. 9, 425 (1960).

[3]D. Sperber, Phys. Rev. 151, 788 (1966).

[4]T. D. Thomas, Annu. Rev. Nucl. Sci. 18, 343 (1968).

[5]W. J. Knox, A. R. Quinton, and C. E. Anderson, Phys. Rev. 120, 2120 (1960); H. C. Britt and A. R. Quinton, *ibid.* 124, 877 (1961).

[6]B. N. Kalinkin and I. Z. Petkov, Acta Phys. Polon. 25, 265 (1964).

[7]S. Cohen, F. Plasil, and W. J. Swiatecki, in *Proceedings of the Third Conference on Reactions between Complex Nuclei,* edited by A. Ghiorso, R. Diamond, and H. Conzett (Univ. of California Press, Berkeley and Los Angeles, 1963), p. 325.

[8]M. Blann and F. Plasil, Phys. Rev. Lett. 29, 303 (1972).

[9]R. Bimbot, M. Lefort, and A. Vigny, J. Phys. (Paris) 29, 563 (1968).

[10]L. Kowalski, J. G. Jodogne, and J. M. Miller, Phys. Rev. 169, 894 (1968).

[11]J. B. Natowitz, Phys. Rev. C 1, 623 (1970); J. B. Natowitz, E. T. Chulick, and M. N. Namboodiri, *ibid.* 6, 2133 (1972).

[12]J. Galin, D. Guerreau, M. Lefort, and X. Tarrago, J. Phys. (Paris) 32, 7 (1971).

[13]F. Pühlhofer and R. M. Diamond, Nucl. Phys. A191, 561 (1972).

[14]A. M. Zebelman and J. M. Miller, Phys. Rev. Lett. 30, 27 (1973).

[15]C. E. Hunting, Phys. Rev. 123, 606 (1961).

[16]F. E. Durham and M. L. Halbert, Phys. Rev. 137, 850 (1965).

[17]J. Beneviste, G. Merkel, and A. Mitchell, Phys. Rev. 174, 1370 (1968).

[18]C. Brun, B. Gatty, M. Lefort, and X. Tarrago, Nucl. Phys. A116, 177 (1968).

[19]R. C. Reedy, M. J. Fluss, G. E. Herzog, L. Kowalski, and J. M. Miller, Phys. Rev. 188, 1771 (1969).

[20]E. H. Auerbach, BNL report ABACUS 2, modified program by B. Donelly and H. C. Chow.

[21]E. H. Auerbach and C. E. Porter, *Proceedings of the Third Conference on Reactions between Complex Nuclei* (see Ref. 7), p. 19.

[22]The targets were obtained from Materials Research Corporation, New York 10962.

[23]G. S. Mani, M. A. Melkanoff, and I. Iori, CEA Report No. 2379, 1963 (unpublished).

[24]J. R. Huizenga and G. Igo, Nucl. Phys. 29, 462 (1962).

[25]D. C. Williams and T. D. Thomas, Nucl. Phys. A92, 1 (1967).

[26]M. J. Fluss, J. M. Miller, J. M. d'Auria, N. Dudey, B. M. Foreman, Jr., L. Kowalski, and R. C. Reedy, Phys. Rev. 187, 1449 (1969).

[27]J. M. d'Auria, M. J. Fluss, G. Herzog, L. Kowalski, J. M. Miller, and R. C. Reedy, Phys. Rev. 174, 1409 (1968).

[28]C. Cabot, thèse de 3ème cycle, Orsay, 1972 (unpublished).

[29]J. Péter, private communication; C. Cabot, C. Ngô, J. Péter, B. Tamain, to be published.

[30]J. B. Grover and J. Gilat, Phys. Rev. 157, 814 (1967).

[31]J. Wilczynski, to be published.

[32]J. Galin, B. Gatty, D. Guerreau, C. Rousset, U. Schlotthauer-Voos, and X. Tarrago, to be published.